Model-Based Segmentation of Surfaces Using Illumination Series

Christoph Lindner, *Student Member, IEEE*, and Fernando Puente León, *Senior Member, IEEE*

Abstract—Automated visual inspection of surfaces plays an important role in the context of industrial production. Segmentation is a key method in image processing of such surfaces. The appearance of structured surfaces depends very much on their illumination. Hence, we apply an illumination that is variable in its direction and in its shape. Image series are taken by varying the direction of the illumination pattern. The segmentation is performed on this data basis. We present an approach that utilizes the Torrance and Sparrow model to estimate the local reflection properties of the surface. The parameters of this model are then used as features to classify each surface point individually.

Index Terms—Automatic optical inspection, image segmentation, lighting control, optical reflection, rough-surfaces measurement, surface-quality measurement.

I. INTRODUCTION

THE QUALITY control of surfaces plays an important role in industrial manufacturing. A surface can have a technical function, e.g., in motor cylinders, or it can influence the customer's purchase decision when it is responsible for the aesthetics of the product. Automated visual inspection (AVI) of surfaces can provide a reproducible accuracy and is easily integrable into the assembly line. Its goal is to detect defects or to measure or analyze patterns and textures [1], [9]–[11]. The segmentation of the surface is a typical and important stage of the signal processing within AVI.

The objective of segmentation is to divide a surface into disjoint regions, each of which is defined by a set of surface properties. These can be, for instance, the local orientation, the color, or the local reflectance properties, as well as neighborhood relations in the spatial domain. This paper presents a method to perform such segmentation based on an illumination series, by which we denote a series of images taken with directional light from different directions. An illumination series contains information about the radiance of the surface as a function of the illumination direction [2], [5], [10]. From this signal, we can derive parameters to use them as features for image segmentation.

Standard segmentation methods on single images assign each pixel to a certain segment according to a defined feature. In the simplest case, this feature is the gray value (or color value,

respectively) of a single pixel. The information contained in a single pixel is limited why more complex segmentation algorithms derive features from neighborhood relations. Examples are the local gray value or the local variance. In addition, previously applied filtering causes neighborhood relations. The consequence is a general loss of spatial accuracy or spatial information. The data basis for the proposed surface segmentation is an illumination series that provides an illumination-dependent signal for each location on the surface, which is mapped onto a pixel of the sensor. For this reason, we can construct a set of model-based features individually for each location on the surface and independently of surrounding locations. We show that a model parameter is a sufficient feature for surface segmentation. However, neighborhood-based filtering is still an option for further enhancements.

Our approach is based on features related to the macrostructure (the local orientation) and to reflection properties caused by the microstructure of the surface. These aspects of surface analysis are partially addressed by photometric-stereo techniques. In its original formulation by Woodham [15], photometric stereo aims to determine the local surface orientation with the help of three light sources, which illuminate the scene from different directions. This method demands prior knowledge on the reflectance properties of the surface, which are specified in so-called reflectance maps. A reflectance map represents the measured local intensity as a function of the surface gradient $[p \; q]^{\mathrm{T}}$ for a fixed illumination direction. Woodham introduced photometric stereo for Lambertian reflectance maps. Tagare and deFigueiredo [13] presented an extension of this technique for a wide class of diffuse non-Lambertian reflectance maps and investigated the sufficient number of illumination directions for a full reconstruction of the surface. Nayar *et al.* [7] developed a method to measure the local orientation and the reflection properties of a surface. The experimental setup utilizes a light source with a certain spatial extent, which corresponds to a superposition of neighboring point-light sources. The effect is a convolution of the illumination function with the bidirectional reflectance-distribution function (BRDF). They showed how the diffuse contribution could be separated from the (glossy) forescatter-reflection lobe.

Photometric stereo and most of its extensions assume a surface with position-invariant reflection properties. This is, however, not the case for many technical surfaces. Moreover, segmentation methods that postulate position-dependent reflection properties cannot be based on these methods. For this reason, most photometric-stereo techniques are not suitable to segment surfaces with location-dependent reflection properties.
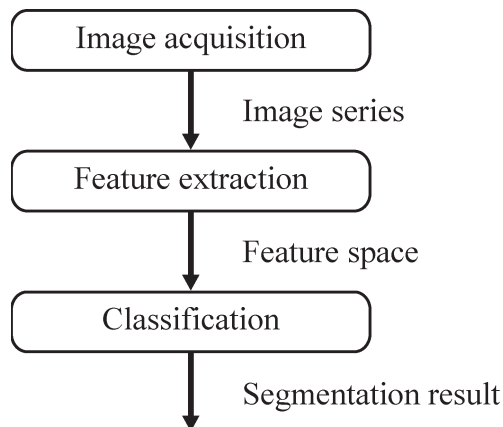
Fig. 1.   General segmentation scheme.

Fig. 2.   Illumination space, spanned by two angles: the azimuth φ and the elevation angle θ. The illumination is performed by a distant point-light source, whose position is defined by the vector $\mathbf{i}$. The observation vector $\mathbf{r}$ typically coincides with the z-axis.

The proposed method can be considered as an implementation of a generalized algorithm for segmentation, as illustrated in Fig. 1. The signal acquisition constitutes the first stage. It is essential to generate signals that carry the desired information about the surface. This is achieved by the choice of a sufficient illumination strategy. Unlike traditional photometric stereo, the illumination strategy must take a spatially varying isotropic BRDF into account. For a fair performance of the method, the number of illumination directions should be kept as low as possible. On the other hand, a minimum number of samples of the illumination space is required to reconstruct the reflection-model function with a predetermined quality. This issue was addressed by Sato *et al.* [12], who applied the sampling theorem on the two-sphere with the help of spherical harmonics. For our algorithm, the simpler case of sampling a 1-D signal is sufficient, as will be shown in the following sections.

The image-acquisition procedure provides an illumination series which builds the source for the feature extraction, which is the second stage of Fig. 1. In this paper, a model-based approach is suggested. The parameters of the Torrance and Sparrow model for surface reflection are employed as features [14]. Another choice would be to take properties of the intensity signal, e.g., the first and the second harmonics [4].

Each pixel, which represents a discrete surface position, is mapped into the feature space, which is spanned by all features. The final stage of the segmentation algorithm is the classification of the features. Even simple linear classifiers can provide reasonable results [4]. More complex or learning classifiers are promising. In addition, a hierarchical classification can be performed. The segments are represented by certain clusters in the feature space. The final segmentation result is obtained when each pixel is assigned to the appropriate class.

Recently, Hertzmann and Seitz [3] presented a segmentation approach based on template matching. The method compares intensity signals of the analyzed surface to those of previously measured templates and performs the segmentation according to the matches. McGunnigle and Chantler [6] presented a surface segmentation based on the surface derivatives and the original intensity of the single images. The surface orientation is estimated by an empirical photometric method. The follow-

ing aspects distinguish our approach from previously published methods.
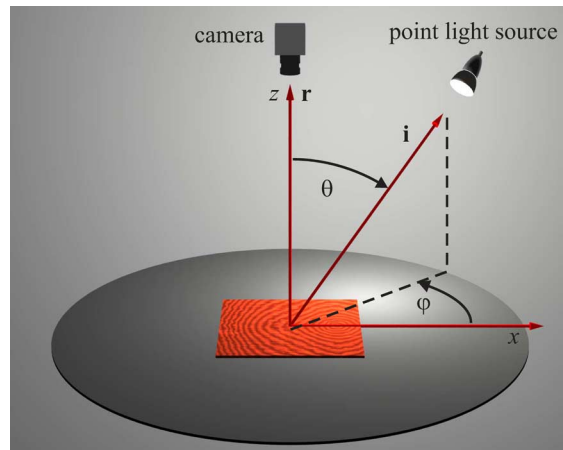
1) An illumination strategy enables the reduction of the number of samples, such that a high accuracy is still obtained for isotropic materials.
2) Reflection model parameters are applied as features.
3) Simple linear classifiers provide satisfactory results for our examples.

Subsequently, we will use the nomenclature on local or surface position to address a discrete area, which is just mapped onto a single pixel of the sensor.

II. PROPOSED APPROACH

A. Illumination Strategy

The choice of a suitable surface illumination is one of the key aspects for the subsequent theoretical and practical discussions. Our experimental setup is characterized by a fixed camera position with its optical axis typically parallel to the z-axis of the global Cartesian coordinate system. The camera lens is assumed to perform a simplified orthographic projection. The illumination space is defined as the space of possible illumination directions and is spanned by two angles: the azimuth φ and the elevation angle θ (see Fig. 2).

An illumination series is a set $\mathcal{D}$ of N images $d(\mathbf{x}, \boldsymbol{\omega}_i)$, which is taken by the camera under different illumination conditions

$$\mathcal{D} = \{d(\mathbf{x}, \boldsymbol{\omega}_n), \qquad n = 0, \ldots, N-1\} \qquad (1)$$

where the vector $\mathbf{x} = (x, y)^{\mathrm{T}}$ describes the location on the surface. The illumination is performed by a distant directional point-light source, whose position is characterized by the parameter vector $\boldsymbol{\omega} = (\varphi, \theta)^{\mathrm{T}}$. The actual illumination parameters represent a discrete subset of the illumination space, and the acquisition of an image series can be considered as a sampling of the illumination space. The intensity signal $g_{\mathbf{x}}(\boldsymbol{\omega})$ describes the intensity of a fixed location $\mathbf{x}$ as a function of the
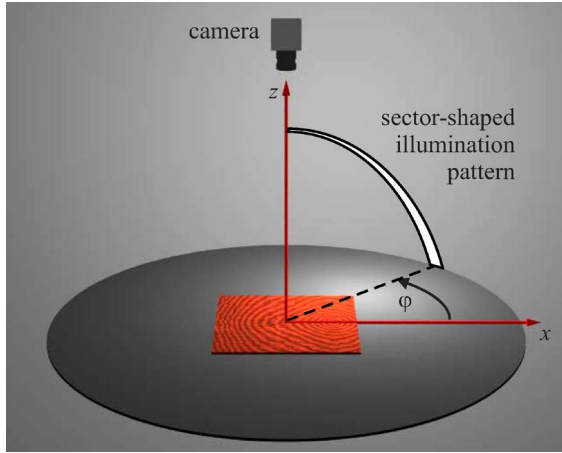
Fig. 3. Sector-shaped illumination pattern consists in a superposition of point-light sources within the illustrated area. With it, an image series can be created as a function of the azimuth φ.

illumination parameters $\boldsymbol{\omega}$. It can be extracted from any illumination series

$$g_{\mathbf{x}}(\boldsymbol{\omega}) := d(\mathbf{x}, \boldsymbol{\omega}). \tag{2}$$

The measured intensity signals $g_{\mathbf{x}}(\boldsymbol{\omega})$ obtained for each location $\mathbf{x}$ on the surface represent the basis for the subsequent steps of the segmentation process.

Besides point-light sources, we also use variable illumination patterns to generate illumination series. The term illumination pattern is referred to as any superposition of point-light sources. The algorithm described as follows utilizes sector-shaped patterns to illuminate the surface from all elevation angles in the interval $\theta_{\mathrm{i}} \in [0°, 90°]$ from an arbitrary azimuth angle φ (see Fig. 3). Consequently, an image series, which is taken with such a pattern, yields intensity signals $g_{\mathbf{x}}(\varphi)$ that solely depend on the azimuth φ.[1]

B. Reflection Model

In this paper, model-based features are used for surface segmentation. The reflection properties of the surface are estimated using the Torrance and Sparrow model, which is suitable for a wide range of materials [14].

The illumination strategy of the measurement algorithm allows a data fit to the model in one dimension. It has taken advantage of the fact that the model and, as a consequence, the segmentation method is limited to isotropic surfaces. The constraints are that the observation direction $\mathbf{r}$, the illumination direction $\mathbf{i}$, and the normal vector $\mathbf{n}$ of the observed surface position $\mathbf{x}$ are in-plane. On this basis, an image series that only depends on the elevation angle θ_{i} can be taken if negative values for the elevation angles are allowed.

The reflected radiance from the surface L_{r} detected by the camera is assumed to be a superposition of a diffuse lobe L_{d} and a forescatter lobe L_{fs}

$$L_{\mathrm{r}} = \lambda_{\mathrm{d}} \cdot L_{\mathrm{d}} + \lambda_{\mathrm{fs}} \cdot L_{\mathrm{fs}}. \tag{3}$$

---

[1]In the following, such a series will be referred to as a φ illumination series.
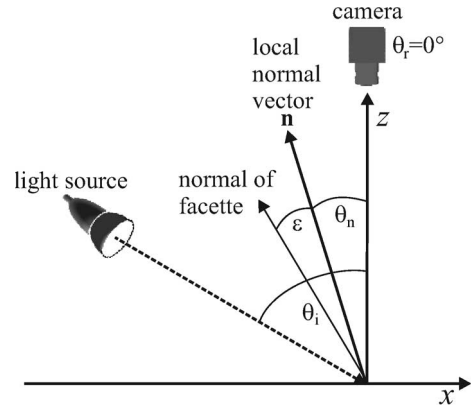
Fig. 4. Illumination direction, direction of observation, and local surface normal $\mathbf{n}$ are in-plane for the applied 1-D case of the reflection model. The facette, which reflects incident light into the camera, is tilted by ε with respect to the normal of the local surface patch.

The parameters λ_{d} and λ_{fs} denote the strength of both factors. The diffuse reflection is modeled by Lambert's cosine law and only depends on the angle of incident light on the surface position

$$L_{\mathrm{d}} = k_{\mathrm{d}} \cdot \cos(\theta_{\mathrm{i}} - \theta_{\mathrm{n}}). \tag{4}$$

The assignment of the variables θ_{i} and θ_{n} is explained in Fig. 4. The forescatter reflection is described by a geometric model according to Torrance and Sparrow [14]. The surface is considered to consist of many microscopic facets, which diverge from the local normal vector $\mathbf{n}$ by the angle ε. Each facet reflects incident light like a perfect mirror. The facets are normally distributed, and the distribution function is rotationally symmetric, because the surface is assumed to be isotropic

$$p_{\varepsilon}(\varepsilon) = c \cdot \exp\left(-\frac{\varepsilon^2}{2\sigma^2}\right). \tag{5}$$

The reflected radiance of the surface patch with the orientation θ_{n} can now be written as a function of the incident light from θ_{i} [8], [14]

$$L_{\mathrm{fs}}(\theta_{\mathrm{i}}) = \frac{\kappa_{\mathrm{fs}}}{\cos(\theta_{\mathrm{r}} - \theta_{\mathrm{n}})} \exp\left(-\frac{(\theta_{\mathrm{i}} + \theta_{\mathrm{r}} - 2\theta_{\mathrm{n}})^2}{8\sigma^2}\right). \tag{6}$$

The parameter σ denotes the standard deviation of the facets' deflection, and it is used as a feature to describe the degree of specularity of the surface. The observation direction of the camera θ_{r} is constant for an image series and is typically set to $0°$. Further effects of the original facette model of Torrance and Sparrow, such as shadowing effects between the facettes, are not considered or simplified in the constant factor k_{fs}.

The reflected radiance L_{r} leads to an irradiance landing on the image sensor. For constant small solid angles, it is allowed to assume that the radiance L_{r} is proportional to the intensities detected by the camera, i.e.,

$$g(\theta_{\mathrm{i}}) \propto L_{\mathrm{r}}(\theta_{\mathrm{i}}). \tag{7}$$

Considering (3)–(7), we can formulate our model for the intensity signals detected by the camera as follows:

$$g(\theta_i) = \kappa_d \cos(\theta_i - \theta_n)$$
$$+ \frac{\kappa_{fs}}{\cos(\theta_r - \theta_n)} \exp\left(-\frac{(\theta_i + \theta_r - 2\theta_n)^2}{8\sigma^2}\right). \quad (8)$$

This equation will be subsequently used to model the intensity of a small surface area as a function of the illumination direction. The model parameters κ_d, κ_{fs}, θ_n, and σ are basically suitable to be used as features for segmentation.

C. Sampling the Illumination Space

In practice, the intensity signals $g_{\mathbf{x}}(\theta_i)$ can only be measured for a limited number of discrete illumination angles θ_i. This process can be considered as a sampling of the illumination space. To keep the image-acquisition effort within reasonable limits, it is interesting to know the minimum number of illumination directions necessary to measure the intensity signal with a defined accuracy.

A general approach to describe the sampling of the illumination space in the two-sphere was presented by Sato *et al.* [12]. They proved that a function with a limited bandwidth σ needs a minimum of $4\sigma^2$ sampling points to be detected. However, finding the correct set of illumination directions to reconstruct the reflection function remains a problem. In this contribution, the sampling problem is simplified to the 1-D case, since this is sufficient for the introduced algorithm. The sampling is performed on a semicircle, which can be described as a function of the elevation angle θ_i, while the azimuth φ is kept constant, as described above. In the case of a pure forescatter reflection, the intensity signals feature a Gaussian shape according to our reflectance model and are, thus, not band-limited. In an attempt to minimize the number of images taken under different elevation angles, it is necessary to know how many sampling points are needed to measure the intensity signal with a predetermined accuracy. To this end, we use Shannon's sampling theorem. The Fourier transform of the forescatter contribution of the intensity signal is given as follows:

$$\mathcal{F}\left\{\kappa_{fs} \exp\left(-\frac{(\theta_i + \theta_r - 2\theta_n)^2}{8\sigma^2}\right)\right\}$$
$$= \kappa_{fs} 2\sigma\sqrt{2\pi} \exp\left(-\frac{f_{\theta_i}^2}{2\sigma_f^2}\right) \exp\left(-j2\pi f_{\theta_i}(2\theta_n - \theta_r)\right). \quad (9)$$

The variance in the frequency space is defined by $\sigma_f^2 := (16\pi^2\sigma^2)^{-1}$. The resulting spectrum of the forescatter reflection has a Gaussian shape. Since this is not a band-limited function, it cannot be reconstructed exactly. However, alternatively, a bandwidth can be defined which contains most of the spectral energy of this signal, such that a sufficiently accurate reconstruction is achieved. We found a bandwidth of $4\sigma_f$ to provide satisfactory results. According to Shannon's sampling theorem, we obtain

$$\Delta\theta_i = \frac{1}{\Delta f_{\theta_i}} < \frac{1}{4\sigma_f} = \pi\sigma. \quad (10)$$

For the number of samples, i.e., the number of images in the illumination series, we obtain

$$I > \frac{\pi}{\Delta\theta_i} = \frac{1}{\sigma}. \quad (11)$$

In the case of an ideal reflection, i.e., for $\sigma \to 0$, an infinite number of samples would be necessary.

To extract the reflection features from the intensity signals $g_{\mathbf{x}}(\theta_i)$ with sufficient accuracy, *a priori* knowledge on the surface is required. In many applications, this knowledge can be derived from former image series taken from similar objects, or it can be estimated by an algorithm that performs an adaptive sampling of the illumination space.

Fig. 5 shows an image series of a varnished-wood surface featuring defects and areas in which the application of varnish failed. For illumination purposes, a distant point-light source with a varying elevation angle θ_i was utilized. The illumination direction, the direction of observation, and the surface normal are in-plane. In this example, an angle of observation of $\theta_r = 30°$ was chosen. The picture in the center shows the surface under diffuse lighting. The remaining five images were acquired with directional illumination from different angles θ_i. On the right side, two illumination signals $g_{\mathbf{x}}(\theta_i)$, which belong to a correctly varnished and to a defective location, respectively, are depicted. To keep the number of samples low while yielding a high accuracy in the interesting range of illumination directions, a variable sampling rate was utilized such that, around the intensity peak, a higher density of samples was chosen. In the case of not equidistant samples, it is not possible to use Fourier analysis to estimate the minimum number of required samples.

D. Algorithm

The algorithm presented in the following allows a point-by-point segmentation based on the surface orientation and the reflection properties—independently of the neighborhood of a surface position.

In a first step, the algorithm detects the orientation of each small surface area with respect to the azimuth. To this end, a φ illumination series of the surface is recorded with a sector-shaped illumination pattern, as described in Section II-A. The intensity signals $g_{\mathbf{x}}(\varphi)$ extracted from such a series depend only on the illumination azimuth φ. Each intensity value results from a superposition of light sources equally distributed over the range $[0°, 90°]$ for the respective azimuth. In [4], two methods to estimate the local azimuth from these intensity signals were described. Both the phase of the first harmonic and the angle yielding the maximal intensity proved to be good estimates of the orientation. This operation is performed in parallel and individually for each position on the surface based on the data of one sector series.

Next, several image series with a varying elevation angle θ_i are taken. To this end, a point-light source is moved over the surface along a semicircular arc, yielding a sampling of the elevation angle in the interval $[-90°, 90°]$. For each orientation detected in the first step of the algorithm, an elevation series
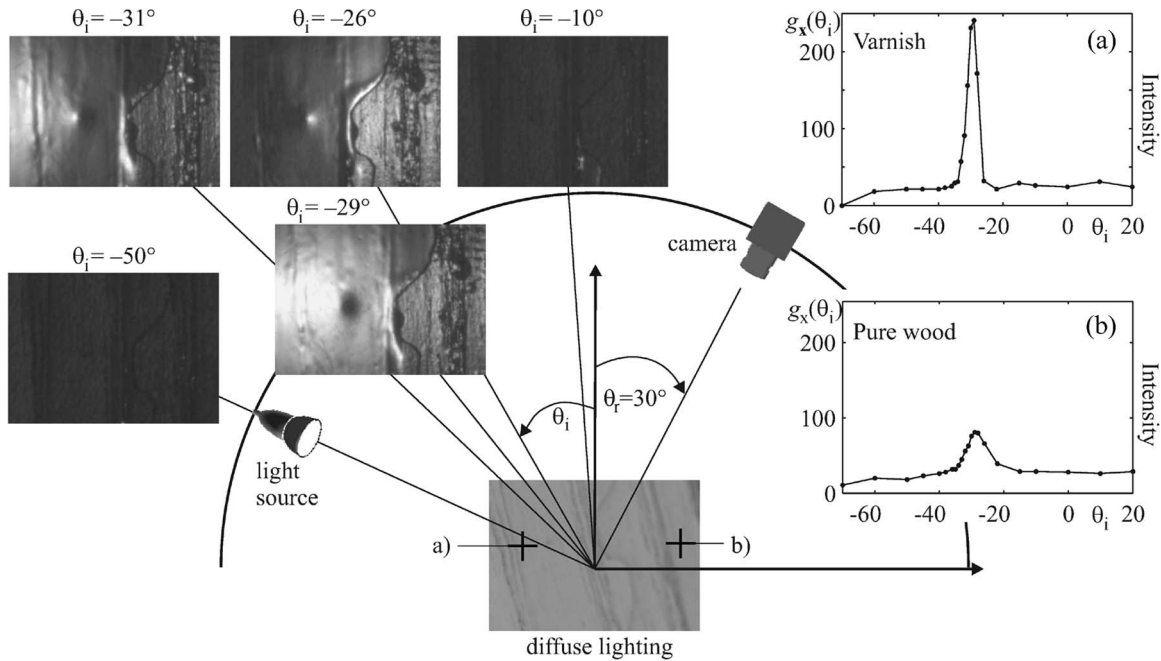
Fig. 5. Elevation series of a partially varnished piece of wood. Images of the object under different illumination directions are displayed on the left side. In the center, the object is displayed under diffuse illumination. (a) The plots on the right side show intensity signals of a highly reflecting varnished location and (b) a failure location, where no varnish was applied and raw wood is affecting the reflection properties.

is acquired by setting the corresponding azimuth. For each location $\mathbf{x}$ of the surface, an intensity signal $g_{\mathbf{x}}(\theta_i)$ with respect to its azimuthal orientation can now be extracted from the series. This intensity signal is a function of the elevation angle and fulfills the requirements of Section II-B, which demand the observation vector, the illumination vector, and the local surface normal to be in-plane.

The reflection properties are then determined individually for each surface location $\mathbf{x}$. For this purpose, the intensity signal is compared to the reflection model, and the model parameters are estimated by fitting the measured intensities to the model based on a minimization of the mean-square distance.

The model parameters can be used as features for segmentation. One or more parameters build a feature space to which standard methods for cluster analysis or classification approaches may be applied. The choice and the setup of these methods control the segmentation, which is the assignment of every location on the surface to a segment. We identified the following parameters as meaningful features:

1) the width of the forescatter lobe σ;
2) the local orientation [4];
3) the relative strength of the Lambertian lobe κ_d and of the forescatter lobe κ_{fs};
4) the sum of the signal samples: $\sum_{\theta_i} g_{\mathbf{x}}(\theta_i)$.

III. RESULTS

The algorithm is demonstrated with a pyramidal metal object with four main sides [see Fig. 6(a)]. Opposite sides of the object have the same surface properties, respectively: sand beamed (top, bottom) or polished (left, right). The sand beamed surface is expected to show a wider forescatter lobe and, thus, a higher value of σ. In contrast, the reflection properties of the polished

surface are closer to the behavior of a mirror. Fig. 6(b), which shows the values of σ coded with gray values, displays this effect. Fig. 6(c) represents the histogram of the width σ of the intensity signals. This distribution features two main modes, which can easily be separated by a threshold, which is chosen manually in this example. Simple linear classifiers such as k-means can be used instead. Alternatively, if the distribution of the segments is known *a priori*, a Bayes classifier can identify the optimal threshold. The number of segments featuring different reflection properties were assumed to be known *a priori*. Fig. 6(d) shows the segmentation result. The different areas corresponding to the sand-beamed and the polished faces could be segmented very well. The sand-beamed areas show highly reflecting spots. This is due to the inhomogeneous surface. The 3-D plot in Fig. 6(e) was reconstructed from the measured surface normal $(\varphi_{\max}, \theta_n)$. The surface intensities correspond to the segmentation result.

Finally, we used the proposed algorithm to detect defects on varnished wood. The defects originate from a lack of varnish or from impurities. In this example, the angle of observation was set to $\theta_r = 30°$. An acquisition of a φ illumination series was not necessary in this case. In Fig. 5, an elevation series is shown. With diffuse lighting, the faultless areas and the defects cannot be distinguished, as can be seen in the image in the center of this figure. On the right side, two plots of intensity signals illustrate the typical differences in the reflection properties between the two surface classes. Fig. 5(a) shows a distinct narrow peak, which is typical for a mirroring varnished surface. The peak of a wooden area is significantly wider and lower [see Fig. 5(b)]. The model-based feature extraction yields the width σ of the peak. This feature is sufficient to distinguish the two classes. Fig. 7 shows the segmentation process. In the top image, the peak width σ was coded with gray values for each location.
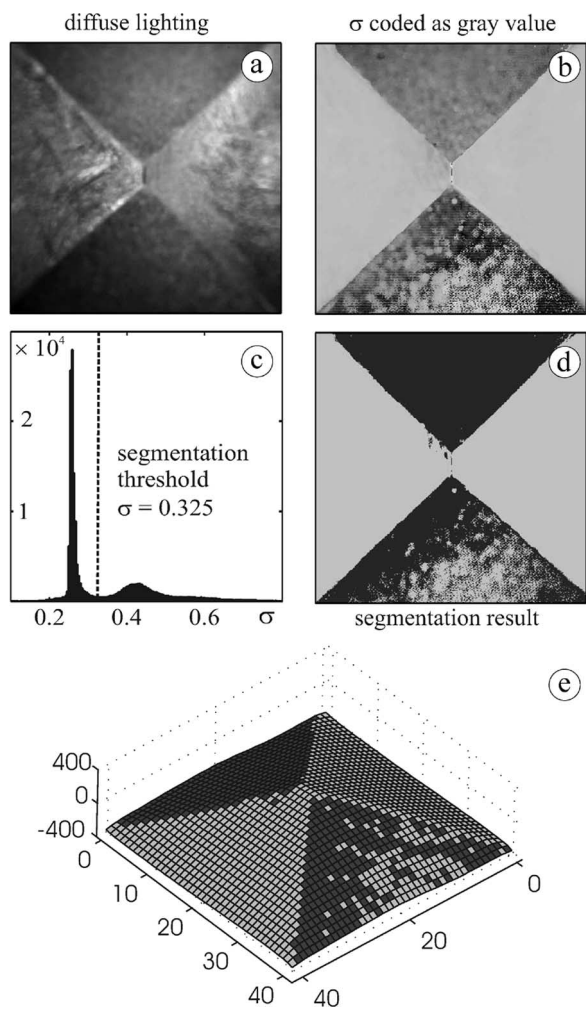
Fig. 6. Segmentation of a pyramidal test object featuring four areas with two different reflection properties and different orientation. (a) Diffuse lighting; (b) width σ of the forescatter lobe coded with gray values for each location; (c) histogram of σ; (d) binary image showing the segmentation result; and (e) 3-D reconstruction based on the measurement data (the surface intensities describe the segmentation result).

The left area is brighter and more homogenous and represents the varnish, whereas, on the right side, the wooden surface appears in a darker hue. The dark spot within the varnished area represents an impurity, which is enclosed in the varnish layer. The histogram of the width σ of the forescatter lobe in the center of Fig. 7 features two modes, representing the two classes varnish (left peak) and wood or defects (right peak). The distribution of the mode representing the wooden surface and the defects is much wider, as this class is less homogeneous than the intact varnish. The two classes can be separated by a threshold, which was done manually. The binary result is depicted in the bottom image of Fig. 7. With the proposed method, both the wooden surface and the impurity defect in the varnish could be discerned from the intact varnish without exploiting neighborhood operators.

Further experiments showed that the method works generally well for segments with reflection properties that feature distinct modes in the histograms, which depends on the difference of reflection functions and on the number of illumination samples. Although the width of the forescatter lobe showed the most
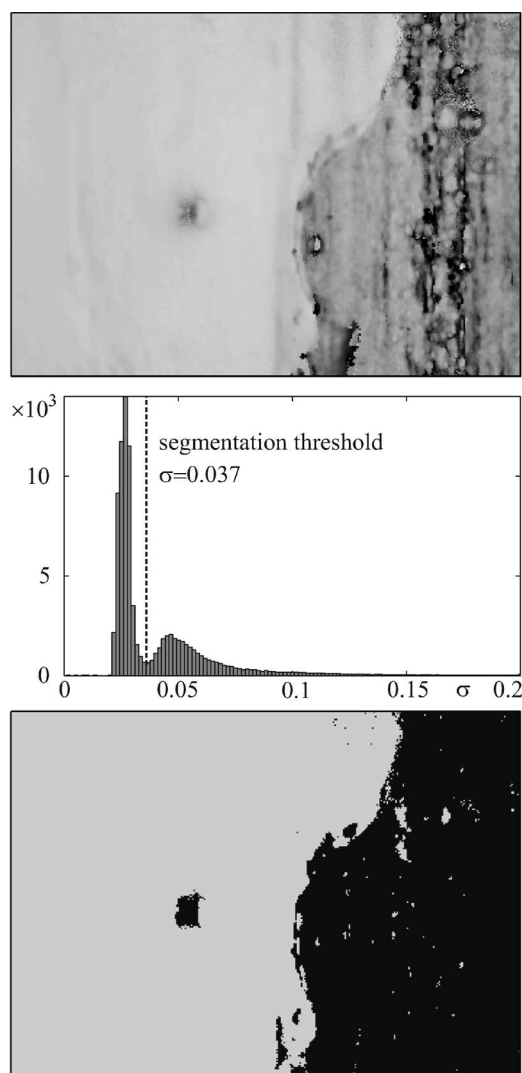
Fig. 7. Varnished piece of wood with areas in which no varnish was applied (defect). The top image shows the measured width σ of the forescatter lobe coded with gray values. The distribution of σ is displayed in the middle plot, and the threshold used for the segmentation is indicated. The bottom plot shows the binary-segmentation result.

promising results, it is also possible to include the other model parameters in the feature vector, which will be subject to future experiments.

IV. CONCLUSION

Structured surfaces can successfully be segmented using illumination series. Such series of images contain significantly more information about the surface characteristics than single images. Particularly, features describing the reflectance properties cannot be derived from a single image. We showed that a model-based approach enables the extraction of descriptive features that can be used to perform a reliable segmentation point by point. However, the expenses of using a model are high. An illumination strategy to sample the illumination space in a suitable manner is required. To estimate the model parameters with sufficient accuracy, a minimum number of samples is needed.

REFERENCES

[1] J. Beyerer and F. Puente León, "Bildoptimierung durch kontrolliertes Aktives Sehen und Bildfusion," *Automatisierungstechnik*, vol. 53, no. 10, pp. 493–502, 2005.

[2] R. M. Haralick and L. G. Shapiro, *Computer and Robot Vision*, vol. II. Reading, MA: Addison-Wesley, 1992.

[3] A. Hertzmann and S. M. Seitz, "Example-based photometric stereo: Shape reconstruction with general, varying BRDFs," *IEEE Trans. Pattern Anal. Mach. Intell.*, vol. 27, no. 8, pp. 1254–1264, Aug. 2005.

[4] C. Lindner, J. Arigita and F. Puente León, "Illumination-based segmentation of structured surfaces in automated visual inspection," in *Proc. SPIE—Optical Measurement Syst. Industrial Inspection IV*, W. Osten, C. Gorecki and E. Novak, Eds., 2005, vol. 5856, pp. 99–108.

[5] C. Lindner and F. Puente León, "Reflection-based surface segmentation using active illumination," in *Proc. IEEE Instrum. Meas. Technol. Conf.*, 2006, pp. 157–162.

[6] G. McGunnigle and M. J. Chantler, "Segmentation of rough surfaces using reflectance," in *Proc. Brit. Mach. Vis. Conf.*, 2001, pp. 323–332.

[7] S. K. Nayar, K. Ikeuchi, and T. Kanade, "Determining shape and reflectance of Lambertian, specular, and hybrid surfaces using extended sources," in *Proc. Int. Workshop Ind. Appl. Mach. Intell. Vis.*, 1989, pp. 169–175.

[8] S. K. Nayar, K. Ikeuchi, and T. Kanade, "Surface reflection: Physical and geometrical perspectives," *IEEE Trans. Pattern Anal. Mach. Intell.*, vol. 13, no. 7, pp. 611–634, Jul. 1991.

[9] A. Pérez Grassi, M. A. Abián Pérez, F. Puente León, and R. M. Pérez Campos, "Detection of circular defects on varnished or painted surfaces by image fusion," in *Proc. IEEE Int. Conf. Multisensor Fusion Integr. Intell. Syst.*, 2006, pp. 255–260.

[10] F. Puente León, "Enhanced imaging by fusion of illumination series," in *Proc. SPIE—Sensors, Sensor Systems, Sensor Data Processing*, O. Loffeld, Ed., 1997, vol. 3100, pp. 297–308.

[11] J. Racky and M. Pandit, "Active illumination for the segmentation of surface deformations," in *Proc. IEEE Int. Conf. Image Process.*, 1999, pp. 41–45.

[12] I. Sato, T. Okabe, Y. Sato, and K. Ikeuchi, "Appearance sampling for obtaining a set of basic images for variable illumination," in *Proc. 9th IEEE Int. Conf. Comput. Vis.*, 2003, pp. 800–807.

[13] H. D. Tagare and R. J. P. deFigueiredo, "A theory of photometric stereo for a class of diffuse non-Lambertian surfaces," *IEEE Trans. Pattern Anal. Mach. Intell.*, vol. 13, no. 2, pp. 133–152, Feb. 1991.

[14] K. E. Torrance and E. M. Sparrow, "Theory for off-specular reflection from roughened surfaces," *J. Opt. Soc. Amer.*, vol. 57, no. 9, pp. 1105–1114, 1967.

[15] R. J. Woodham, "Photometric method for determining surface orientation from multiple images," *Opt. Eng.*, vol. 19, no. 1, pp. 139–144, 1980.

Christoph Lindner (S'06) was born in Munich, Germany. He received the degree in electrical engineering from Friedrich Alexander University, Erlangen, Germany, and the degree in information and communication technology from the Technische Universität München, München, Germany. In 2003, he wrote the Diploma thesis at the Centre of the Neural Basis of Hearing, Cambridge, U.K. He is currently working toward the Ph.D. degree at the Department of Electrical Engineering and Information Technology, Technische Universität München.

His research interests are focused on image processing and psychoacoustics.

Fernando Puente León (S'94–M'99–SM'06) received the M.S. degree in electrical engineering and the Ph.D. degree in automated visual inspection from the University of Karlsruhe, Karlsruhe, Germany, in 1994 and 1999, respectively.

From 2001 to 2002, he was employed by Design of Systems on Silicon, Valencia, Spain. From 2002 to 2003, he was a Postdoctoral Research Associate at the Institut für Mess-und Regelungstechnik, University of Karlsruhe, where he headed the Information Fusion Group. He is currently a Professor with the Department of Electrical Engineering and Information Technology, Technische Universität München, München, Germany. His research interests include image processing, automated visual inspection, information fusion, measurement technology, pattern recognition, and communications.